ISPRS Int. J. Geo-Inf. **2015**, *4*, 900-927; doi:10.3390/ijgi4020900

OPEN ACCESS

ISPRS International Journal of

Geo-Information

ISSN 2220-9964

www.mdpi.com/journal/ijgi/

Article

Mapping the Socio-Economic and Ecological Resilience of Japanese Coral Reefscapes across a Decade

Antoine Collin [1,2,*], Kazuo Nadaoka [1,†] and Lawrence Bernardo [1,†]

[1] Department of Mechanical and Environmental Informatics, Tokyo Institute of Technology, Tokyo 152-8552, Japan; E-Mails: nadaoka@mei.titech.ac.jp (K.N.); bernardo.l.aa@m.titech.ac.jp (L.B.)

[2] Department of Life and Earth Sciences, Ecole Pratique des Hautes Etudes, Dinard 35800, France

† These authors contributed equally to this work.

* Author to whom correspondence should be addressed; E-Mail: antoine.collin@ephe.sorbonne.fr; Tel.: +33-2-9946-1072.

Academic Editor: Wolfgang Kainz

Received: 13 February 2015 / Accepted: 12 May 2015 / Published: 26 May 2015

Abstract: Shallow coral reefs threatened by climate change must be spatio-temporally analyzed in terms of their protection of coastal human populations. This study combines Japanese spatio-temporal gradients of population/asset and coral buffering exposure to stress-inducing and stress-mitigating factors so that the socio-economic and ecological (SEE) resilience tied to coral reefscapes can be regionally mapped (1200 km) at a fine resolution (1 arcsec) over a decade (11 years). Fuzzy logic was employed to associated environmental factors based on the related population/asset/coral buffering responses, as found in the literature. Once the factors were weighted according to their resilience contributions, temporally static patterns were evident: (1) a negative correlation occurs between coral buffering resilience and latitude; (2) the least resilient islands are low-lying, deprived of wide reef barriers, and located on the eastern and southern boundaries of the Nansei archipelago; (3) the southwestern-most, middle and northeastern-most islands have the same SEE resilience; and (4) Sekisei Lagoon islands have a very high coral buffering resilience. To overcome uncertainty, future studies should focus on the socio-ecological adaptive capacity, fine-scale ecological processes (such as coral and fish functional groups) and the prediction of the flood risks in the coming decades.

Keywords: coastal mapping; socio-economic and ecological system; resilience; coral reefs; spatio-temporal; high resolution

---

1. Introduction

Coastal coral reefs, which provide valuable marine-based ecological services to mankind, have become a prominent scientific and socio-economic issue because they are rapidly declining worldwide. These tropical and sub-tropical ecosystems protect coastal populations from high-energy oceanic events, supply seafood, and stimulate recreational activities [1]. Although coral reef services have been valued at approximately US$ 6000 $ha^{-1}\cdot year^{-1}$ [2], 19% of these services have been recently lost [3] as a consequence of anthropogenic stressors, including overfishing, eutrophication, sedimentation, disease and climate change [4,5]. If 15% of the population is seriously threatened within 10–20 years and another 20% becomes threatened in 20–40 years, approximately half will remain healthy and resilient to current threats [3,6]. As an insightful concept to comprehend nonlinear dynamics within complex systems, resilience has been especially of interest to coral reef scientists over the last decade [7–9].

Because of the unprecedented pace of reef loss and climate-mediated threats, coral reef resilience, such as the capacity of scleractinian-regime reefs to successfully tolerate disturbance, has been at the center of the main innovative management programs that operationalize reefs [10–14]. Commonly, the latest literature performs empirical assessments of reef resilience by appropriately measuring the factors that confer and undermine the resilience of coral reefs [15]. These authors provided a foundational framework based on the *in situ* identification of primary benthic covers and morphology, fish functional groups, water column and light properties, and anthropogenic drivers. Although recent practical approaches have identified prime elements of coral reef resilience, their widespread application remains limited because of the use of traditional survey techniques, which document sparse and discrete patches of less than 100 m^2. Techniques suitable for capturing spatial resilience (*i.e.,* spatial heterogeneity and connectivity) in a continuous way are advocated to link spatial patterns of coral reef regimes [10].

Because remotely sensed data are continuous over regions, some studies have recently pioneered their integration into functional coral reef mapping for various purposes. A global model of spatial coral reef exposure, including 11 factors (based on remotely sensed temperature, ultraviolet radiation, wind speed, sedimentation, eutrophication, temperature variability and tidal range), was established to prioritize local management efforts [16]. Although the model clearly informs planning and decision-making at the global scale, its scope is limited by its coarse spatial resolution, which amalgamates spatially and spectrally complex coral reefs into one 4 km resolution pixel. [17] succeeded in mapping three resilience indicators (herbivore functional group richness, living coral and crustose coralline algae, and stress-tolerant coral taxa) at a 4 m resolution using field data scaled up by high-resolution satellite data, but they did not integrate the indicators into a single spatial model suitable for implementing management strategies. With a focus on a 1 km resolution, [18] combined six factors (living coral abundance, framework abundance, water depth variability, fishing, industrial development and temperature stress) into a generic resilience index using high-resolution satellite data and weighted linear combinations. Integrating the social dimension into resilience research has the potential to motivate the local community to engage in the management of ecosystem services [19].

Along with increasingly complex systems, inclusive socio-ecology has naturally grown with the emergence of resilience to elucidate and efficiently consider the dynamics of interactions between people and nature [20–23]. Tipping points and thresholds reflect significant theoretical discoveries related to the resilience of socio-economic and ecological (SEE) systems, particularly in coastal and marine ecosystems [24,25]. Combining spatial approaches to societies and ecosystems is promising for shifting SEE systems toward more sustainable states [26] because of the stakeholder involvement triggered by teaching and implementation methods conveyed by mapping products. However, very few applications regarding the spatial resilience of SEE systems have been published [27], particularly in the context of coral reefs.

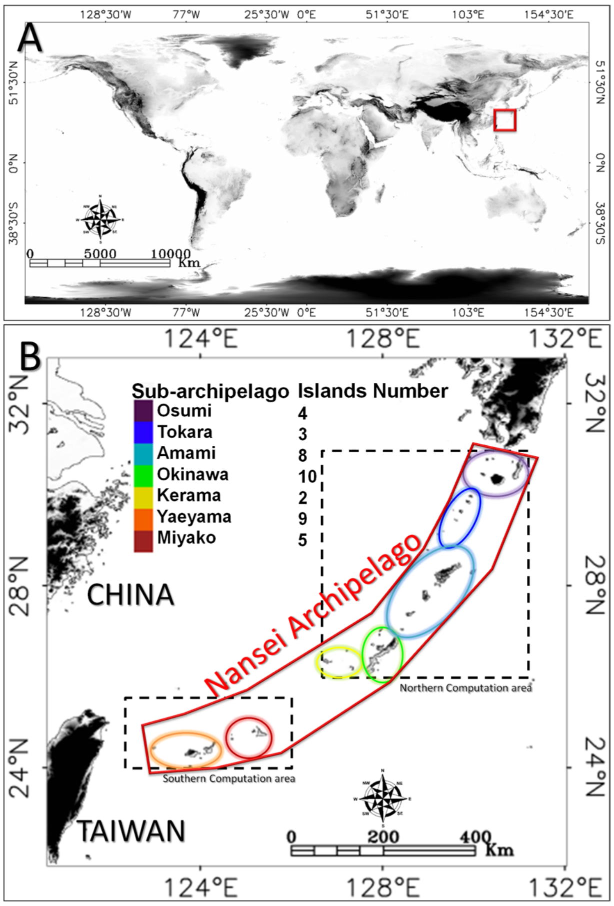

Figure 1. Location maps of the Nansei archipelago in (**A**) Southeast Asia, between (**B**) Taiwan and southern Kyushu. At 1200 km, the archipelago is composed of seven sub-archipelagoes and is examined as two study areas: northern and southern areas comprising five and two sub-archipelagoes, respectively.

In this study, we map the spatial resilience of SEE systems associated with coral reefs across a large region (~1200 km length) at the highest spatial resolution possible (1 arcsec, approximately 30 m). All of the Japanese islands with shallow coral reefs (*i.e.*, Nansei archipelago, Figure 1) are considered. Our study focuses on a suite of 19 spatialized endogenous, exogenous stress-inducing and stress-mitigating factors derived from freely available spaceborne and waterborne observations, model output, historical databases and census data. Because of the uncertainty inherent in the knowledge of society–coral–environment interactions, we transform factor layers to fuzzy logic measures [28] and assemble them into single socio-economic and single ecological resilience metrics. By processing standardized measures of the degree of membership along a continuous gradient, fuzzy logic is much more suitable for modeling complex systems than the traditional binary rule. To create compelling and novel SEE systems mapping products, we compute the spatial resilience for a decade (2002–2012) with a one year lag. Dynamic patterns of both socio-economic and ecological resilience indicators are analyzed by assessing the average differences at 41 islands, spanning seven sub-archipelagoes.

2. Methods

2.1. Study Region

The study area covers the southwestern Japanese islands, *i.e.*, the Nansei archipelago, between 24°N and 31°N. The area is characterized by coastal coral reefs and terraces of emergent coral reefs. The ocean to the west of the archipelago is greatly influenced by the Kuroshio Current, which drives tropical waters from the Philippines Sea to the East China Sea [29]. The comma-shaped archipelago is ~1200 km long, an average of 150 km wide, 1709 m high and 4623 m deep. Although we focused on 41 islands that were categorized into seven sub-archipelagoes (see Figure 1), the study area spanned two large zones: the southern (~90 km^2) and the northern (250 km^2) Nansei sub-regions (see the black dotted rectangles in Figure 1).

2.2. Linking the Socio-Economy and the Ecology

Methods for spatially assessing coral reef resilience have been developed by determining the primary factors that are stressful for scleractinian-regime reefs and factors that assist those reefs in coping with stress-induced changes [17,18]. To our knowledge, methods for spatially assessing socio-economic and ecological (SEE) resilience tied to coral reefscapes are lacking. We therefore developed a methodology based on the interplay between the SEE fundamentals akin to coastal and coral reefs and the potential of representing critical factors in a spatially explicit manner. To comprehend the complex dynamics of the SEE systems as meaningfully as possible, the SEE components were compared. In addition to the three population/asset/coral buffering endogenous factors, the SEE strands contained four and six stress-inducing factors, respectively, and one and six stress-mitigating (hereafter, “resilient”) factors, respectively (Figure 2).

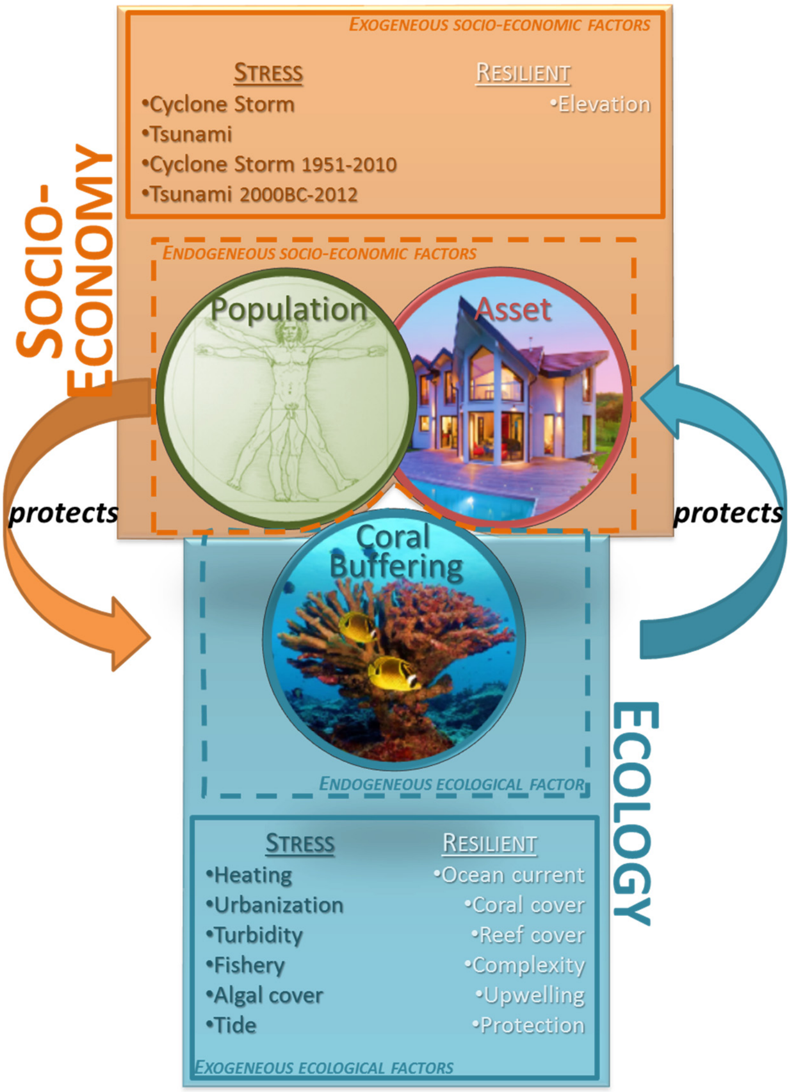

Figure 2. Conceptual framework centered on the endogenous socio-economic (population/asset) and ecological (coral buffering) factors influenced by exogenous stress-inducing and stress-mitigating (resilient) factors.

2.3. Socio-Economic Factors

The Nansei archipelago is particularly suitable for studying socio-economic resilience in a coastal context given the high population density in coastal areas (185–615 inhab·km^{-2}, [30]) and the high frequency of both tropical cyclones (TCs) and earthquake-driven tsunamis [31,32], which greatly strain coastal systems. We used historical databases, spaceborne data and census data to create spatial layers that represent endogenous, exogenous oceano-climatic and elevation factors (Table 1).

Table 1. Socio-economic stress and resilience exogenous factors, space-time data features, weighting and justification of the factors. The justification is rooted in the main references that link the factor with its relevance to the Japanese socio-economic resilience related to coral reefscapes.

Factor		Proxy	Source	Space Resolution	Time Resolution	Weight	Reference
Stressor	Acute climatic hazards	Cyclone Storm	Tropical Cyclone Best-Track data	1 arcsec	2002–2012, 1 year	2	[33]
	Acute oceanic hazards	Tsunami	Global Historical Tsunami Database	1 arcsec	2002–2012, 1 year	2	[34]
	Chronic climatic hazards	Cyclone storm (1951-2010)	Tropical Cyclone Best-Track data	1 arcsec	1951–2010	1	[33]
	Chronic oceanic hazards	Tsunami (2000BC–2012AD)	Global Historical Tsunami Database	1 arcsec	2000BC–2012AD	1	[34]
Resilient	Resistance to oceano-climatic hazards	Elevation	Global Digital Elevation Model (v.2)	1 arcsec	2011	3	[24]

2.3.1. Population and Asset Endogenous Factors

The population and the land price (¥·m^{-2}) constitute two endogenous socio-economic factors [35]. The Nansei population layer was derived from the 2.5 arcmin gridded population of the world distributed by the Socio-Economic Data and Applications Center (http://sedac.ciesin.columbia.edu/gpw). A 1 arcsec linear triangulation map was built for three years, *i.e.*, 2000, 2005 and 2010, which are representative of the three following periods: 2002–2004, 2005–2009 and 2010–2012. The economic asset were retrieved from the Publication of Land Price data (from 1983 to 2012), which are published by the Ministry of Land, Infrastructure, Transport and Tourism Land Appraisal Committee (http://nlftp.mlit.go.jp/ksj-e/gml/datalist/KsjTmplt-L01-v2_1.html).

The asset layer was mapped annually from 2002–2012 on a 1 arcsec grid.

2.3.2. Oceano-Climatic Stress Exogenous Factors

TC- and earthquake-induced surges, also called typhoons and tsunamis in Southeast Asia, respectively, were the two main socio-economic stressors in our study region [33,34].

The TC layers were derived from the tropical cyclone best-track data provided by the Japan Meteorological Agency (http://www.digital-typhoon.org/). This database contains the date and time, central pressure (hPa), and latitude and longitude (y, x with 6 arcmin spatial resolution) measured every 6 hours for each recorded typhoon since 1951. We developed an algorithm to create a layer of TC influences for a specific period. A suite of temporary sub-layers was created based on the 1 arcsec linear triangulation of the 1° buffer area around each sample (hPa, y, x) using IDL-ENVI (Exelis Visual Information Solutions, Boulder, CO, USA). Then, temporary sub-layers were inverted to change the buffer into the influence layer before being summed for a specific period of interest. As a proxy for an acute and chronic climatic stressor, a TC-influence layer was computed for each year from 2002 to 2012 (160 ± 49 sub-layers) and for the 1951–2010 period (5796 sub-layers), respectively.

The tsunami layers were produced from the global historical tsunami database maintained by the National Geophysical Data Center (http://www.ngdc.noaa.gov/hazard/tsu_db.shtml). The array features the year, primary magnitude, and latitude and longitude (y, x with 6 arcmin spatial resolution) of every tsunami recorded since 2000 BC. We attributed a magnitude of 7 to the historical events deprived of any values (*i.e.*, 10 out of 67) insofar as its database identifies major tsunami events. We applied the TC algorithm to tsunamis (1° buffer area) and then built a tsunami-influence layer (1 arcsec spatial resolution) for a specific period. As a proxy for an acute and chronic oceanic stressor, a tsunami-influence layer was created each year from 2002–2012 (tsunamis only occurred in 2002, 2006 and 2010) and for the 2000 BC–2012 AD period (67 sub-layers/events with a 6.88 ± 0.56 magnitude average, from 744–2010 AD).

2.3.3. Elevation Resilient Exogeneous Factor

The sensitivity of the coastal human population to oceano-climatic stressors is intricately linked with the elevation from the shoreline [24]. The elevation layer was extracted from the 5 m mesh digital elevation model distributed by Japan's Geographical Survey Institute in the form of 0.125° × 0.08° tiles at 12 and 0.1 m horizontal and vertical resolutions, respectively (http://fgd.gsi.go.jp/download/). The tiles were combined into a large mosaic, which was spatially re-sampled to a 1 arcsec resolution for spatial consistency with stressors-related products (0.0–1923.2 m range).

2.4. Ecological Factors

Only spaceborne data were used to create spatial layers that embody endogenous and exogenous factors (Table 2).

Table 2. Ecological stress and resilience exogenous factors, space-time data features, weighting and justification of the factors. The justification is based on the main references that link the factor with its relevance to Japanese ecological resilience in relation to coral reefscapes.

Factor			Source	Space Resolution	Time Resolution	Weight	Reference
Stressor	Thermal stress	Heating rate	MODIS SST (11 µm)	4 km	Summer 2002–2012, 1 week	2	[36,37,38]
	Habitat-removal toxicity Algal competition	Urbanization	DMSP-OLS	30 arcsec	2002–2012, 1 year	2	[39,40]
	Sediment stress	Turbidity	MODIS Kd (490 nm)	4 km	2002–2012, 1 year	1	[41,42]
	Algal competition Anchor damage	Fishery	VHR Google Earth Professional	2 m	2013	1	[3,43,44]
	Algal competition	Algal cover	ALOS/AVNIR-2-	10 m	2009–2010	1	[45,46]
	Emersion adjustment	Tide exposure	NAO.99b tidal prediction system/Delft3D	5 arcmin	Spring 2002–2012, 1 day	1	[47,48]
Resilient	Connectivity	Ocean current	MODIS SST (11 µm)	4 km	Winter 2002–2012, 1 week	3	[49,50]
	Coral source	Coral cover	ALOS/AVNIR-2-	10 m	2009–2010	3	[51]

Table 2. *Cont.*

Factor		Source	Space Resolution	Time Resolution	Weight	Reference
Habitat sink	Reef cover	ALOS/AVNIR-2-	10 m	2009–2010	2	[52,53]
Ecological niche	Bathymetric complexity	VHR Google Earth Professional	2 m	2013	2	[54,55]
Thermal cooling	Upwelling	GEBCO 08-grid	30 arcsec	2008	1	[56]
Removal of anthropogenic impacts	Protected Area	Protected Planet	1 arcmin	2013	1	[57]

2.4.1. Coral Buffering Endogenous Factor

As complex shallow coastal forms, coral reefs significantly help cope with coastal hazards first by reducing wave energy and secondly by attenuating the flow velocity [58]. To quantify the ecological protection provided by coral reefs, a customized index combining both the surface area and the resistance force exerted on the flow velocity was established (Table 3). The buffer area was retrieved from the 10 m Coral Reef Habitat Map established by the Japanese Ministry of Environment based on a suite of satellite images acquired in 2008–2009 mainly by the ALOS/AVNIR2. The freely available product is an accurate classification (70%) of Japanese coral reefscapes into seven classes in the form of polygon vectors (http://coralmap.coremoc.go.jp/sangomap_eng/). The buffer area consisted of the spatial junction of polygons pertaining to the six following classes: Coral cover 50%–100%, coral cover 5%–50%, rock, seaweed, sand and mud. Then, a drag coefficient C_d was assigned to each class according to a drag gradient interpolated from the literature [59], and a 1 arcsec coral buffering layer was triangulated for 2002–2012.

Table 3. The drag coefficient for the habitat classes composing Japanese coral reefscapes (derived from [59]).

Habitat Class	Drag Coefficient (C_d)
Coral cover 50%–100%	0.06
Coral cover 5%–50%	0.045
Rock	0.03
Seaweed	0.02
Sand	0.01
Mud	0.01

2.4.2. Stress Exogenous Factors

Thermal and Sediment Stress

Large anomalies in seawater temperature lead to coral bleaching and frequently to coral death [36–38]. Sea surface temperature (SST) data were used to compute an indicator developed and validated as a heating rate index. The indicator basically corresponds to the ratio between the degrees Celsius above the average over the period of interest (high anomaly) and the number of weeks experiencing positive anomalous temperatures. The SST data were retrieved from the 4 km Aqua MODIS 11 μm nighttime product maintained by the National Aeronautics and Space Administration service dedicated to ocean observation (http://oceancolor.gsfc.nasa.gov/). The heating rate index was computed for each year (from 2002–2012) based on the 15 hottest weeks (mid-May to mid-September) and was processed with 1 arcsec linear triangulation.

Poor water clarity due to runoff may be very harmful to coral reefs by depriving them of sunlight and covering them with sedimentation [42]. Applying the computation principles of the heating rate index to the water clarity (hereafter, turbidity), we calculated the ratio between the positive anomalies and the number of weeks experiencing positive turbidity anomalies. Turbidity data were retrieved from the 4 km Aqua MODIS diffuse attenuation coefficient at 490 nm (http://oceancolor.gsfc.nasa.gov/), and a 1 arcsec turbidity layer was built annually for 2002–2012 based on the 46 most turbid weeks (mid-February to mid-November).

Urbanization Stress

Urban sprawl converts natural habitats into concrete areas that are significant sources of pollution for downstream ecosystems, including shallow coral reefs [39,40,42]. Assuming that a correlation exists between urban light intensity at night and the degree of urbanization [60] and that pollutants are advected and diffused into water (the farther from the source, the lower the impact), an urbanization index may be implemented using the Defense Meteorological Satellite Program Operational Line Scan (DMSP-OLS) Nighttime Lights Time Series available from the National Geophysical Data Center (http://www.ngdc.noaa.gov/dmsp/). With an initial 30 arcsec pixel size, an urbanization layer was created for every year from 2002–2012 and was re-sampled at 1 arcsec using linear triangulation.

Fishery Stress

The removal of fish populations, which graze algae, is highly likely to entail an ecological shift in a coral reefscape in favor of the dominance of macroalgae [3,43,44]. We hypothesize that the number of fishery vessels anchored in ports is correlated with the fishery pressure exerted on the reef fish populations [17]. The sizes of the fishing boats commonly found in the Okinawa and Kagoshima prefectures range between 8 and 15 m. Monitoring fishing boats therefore requires access to very-high-resolution (VHR) spatial datasets that can be achieved using the freely available Google Earth geoportal, whose VHR information is based on satellite images gridded between 0.5 and 2.4 m (2002–2012). A total of 441 ports were targeted and 12,798 fishing boats (8302 moored and 4496 on dry docks) were individually counted. Ultimately, 441 sub-layers were obtained, in which each contained a 1° buffer area centered on the port location and weighted by the intrinsic number of vessels. A fishery-influence layer was produced as the sum of the value-inverted sub-layers, triangulated at the 1 arcsec pixel size. Because of the unavailability of time series over some parts of the study area, a single fishery layer was representative of 2002–2012.

Algal Competitor Stress

The cover of algae is a direct measurement of the stress borne by coral reefs because of the competition for space, which is particularly important for coral recruits after a significant disturbance [46]. Algae cover was extracted from the 10 m Coral Reef Habitat Map (see Section 2.4.1.). Sub-layers of 331 polygons related to algal cover were generated as 3 arcsec buffer areas, value-inverted and finally summed in an algal-influence layer. Owing to the single habitat map for 2002–2012, only one algal layer was deemed relevant across this period.

Emersion Adjustment

As marine invertebrates, coral reefs become vulnerable to ultraviolet rays, thermal increases and desiccation when experiencing emersion events [48]. The tidal stress on coral reefs may be properly quantified by the amplitude between low and high tides. A tidal hindcast was conducted using the Delft3D D-Flow program (Deltares systems, Delft, Netherlands) based on the NAO.99b tide prediction system [61] and the 30 arcsec General Bathymetric Chart of the Oceans (GEBCO_08 Grid) released in 2011. Preliminary observations showed that the largest amplitudes regularly occur during the spring in this region. For each year between 2002 and 2012, an initial tide amplitude layer, based on the difference between the highest and lowest tide between mid-February and mid-April, was produced at 30 arcsec and then triangulated at 1 arcsec.

2.4.3. Resilient Exogenous Factors

Connectivity

Considered a primary cause of resilience, connectivity allows post-disturbance coral reefs to benefit from recruits [49]. Kuroshio is a strong western-boundary current that transports recruit-enriched tropical waters northward from the Philippines Sea. Because the spatial patterns of this ecological corridor show spatial heterogeneity in the study area, we confidently assume that Kuroshio main route reflects the large-scale connectivity inherent to this region. Specifically, the Kuroshio Current is more easily detectable in the cold season than in the hot season due to the large SST gradient. Connectivity data were retrieved from the 4 km Aqua MODIS SST 11 μm nighttime product (http://oceancolor.gsfc.nasa.gov/), and a 1 arcsec connectivity layer was built annually for 2002–2012 based on the average of the 12 weeks of winter (mid-December to mid-March).

Coral Source and Habitat Sink

The ecological source of self-recruited and disturbance-recruited corals is another key factor of the coral reef resilience [51]. Moreover, habitat sinks, which are devoid of coral competitors, appear essential for hosting new recruits and expanding the living coral [52]. The coral and reef cover mapped into the 10 m Coral Reef Habitat Map (see Section 2.4.1.) suitably represent the coral sources and habitat sinks. The coral classification distinguished two living coral classes: 5%–50% and 50%–100% living-coral covers. Sub-layers of 551 (462 and 89) and 1794 polygons related to coral sources and habitat sinks, respectively, were generated as 3 arcsec buffer areas, value-inverted and finally summed as coral-source and habitat-sink layers. Given the putative difference in the recruit supply between the two coral sources, we weighted the 5%–50% and 50%–100% classes by 0.5 and 1 before the summation. Similar to the algal layer, a single coral source and a single habitat sink layer were created for 2002–2012.

Ecological Niche

The physical complexity of the coral reefscape provides a wide range of habitats at various scales. Shading during intense solar radiation episodes protects coral colonies and recruits from bleaching by alleviating highly fluctuating temperatures [54,55]. The bathymetric complexity can be satisfactorily captured by assessing the horizontal spatial variability in the water depths found in the reefscape. Given the spatial scale at which ecological processes interact with coral colonies, a high-resolution bathymetry and complexity assessment is required. In contrast to the 30 arcsec GEBCO_08 Grid, Google Earth is likely to furnish high-resolution (2 m) data (see Section 2.4.3.), pending a methodology that can extract water depths from natural-colored images. Drawing on our recent results that suggest Google Earth images may adequately render the bathymetry ($R^2 \approx 0.7$, see [62]), we formed a mosaic of georeferenced Google Earth images (2.4 m) at an appropriate altitude for the entire study region. We then derived the water depths using the blue-red ratio transform, and we computed the subsequent data range of the water depths before re-sampling at 1 arcsec using a 3 × 3 kernel size. Considering the time lapse of change in the bathymetry and the lack of time series over some parts of the study area, a single ecological niche layer was created for 2002–2012.

Thermal Cooling

The hydrodynamic connection of coral reefs to deeper and cooler bodies of water is a great asset to attenuate the deleterious, even lethal, effects of water temperature increases [56]. The spatial proximity of shallow coral reefs with deeper bottoms is necessary for the ascent of deeper and cooler water toward coastal areas; this phenomenon is known as upwelling. Thermal cooling can be reliably quantified using the distance of significant slopes along the Ryukyu Arc on the 30 arcsec GEBCO_08 Grid. We computed a 1° buffer area around each of the 97 areas that featured a slope > 13° and summed the value-inverted sub-layers to create a single 1 arcsec thermal-cooling influence layer for 2002–2012.

Coral Protected Area

In addition to the self-organization of the investigated socio-ecosystems, human populations can preserve coral reef ecosystems and their inherent ecological services, including coastal protection. A comparison of approaches to coral reef management indicated that the effective conservation of managed areas significantly surpassed that of unmanaged areas [57]. Because watershed management also has a large influence on coral reefs [42], terrestrial protected areas were jointly examined with marine areas. Surface areas were extracted from the Protected Planet project, which lists the characteristics of 23 areas, including vector data and dates of implementation (http://protectedplanet.net/). Polygons were first rasterized at 1 arcsec and then used to nest 3 arcsec (land) and 0.01° (marine) buffer areas, which were value-inverted and summed to obtain the influence layers. Four coral-sink protection layers were generated for 2002–2012:

- 2002–2004, including 19 protected areas
- 2005–2006, including 20 protected areas (Kerama Shoto Coral Reef implementation)
- 2007–2011, including 21 protected areas (Ishigaki implementation)
- 2012, including 23 protected areas (Hateruma and Hatoma implementation)

2.5. The Fuzzy Logic for the Socio-Economic and Ecological Resilience

A suite of derived factors, endogenous and exogenous (either stress-inducing or stress-mitigating), were considered to capture the spatio-temporal variability in the SEE resilience of coral reefscapes. The interactions of agonistic and antagonistic drivers may be additive and multiplicative, creating complex dynamics, including thresholds that are beyond the reach of any traditional linear models [16]. Fuzzy logic is an insightful methodology to represent the combination of linear and non-linear momentums in measuring the possibility of membership along a continuous scale from 0–1 [28]. A logistic curve was computed as the cumulative normal distribution function between a lower (x_a) and an upper (x_b) bounds along the gradient of each factor. After pairing each of the 17 exogenous factors with the function that better fitted the interaction between them and the endogenous population/asset/coral buffering factors, the logistic curve was selected given its predominance. We thereby assume that the resilience response of the coastal human and natural populations to a stress-inducing exogenous factor is the inverse of an S-shape curve, *i.e.*, the response plateaus at 1 before the minimum threshold, transitionally decreases, exponentially decreases, and then plateaus at 0 (Figure 3A). Conversely, the resilience response to a stress-mitigating exogenous factor may be described by an S-shape function (Figure 3B).

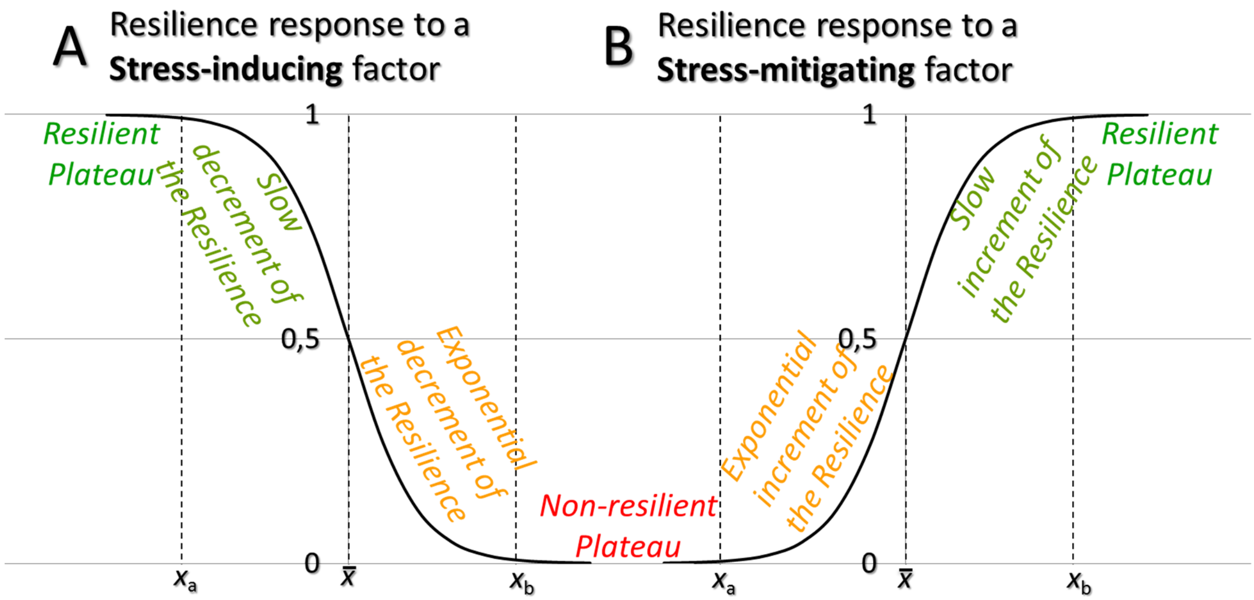

Figure 3. Resilience responses to factors modeled by (**A**) a decreasing logistic function and (**B**) an increasing logistic function when confronted by stress-inducing and stress-mitigating factors, respectively. A sequence of four phases can be described for each function: resilient, slow decrement/increment, exponential decrement/increment, and non-resilient. x_a, x_b and $\bar{x}$ correspond to the minimum, maximum and the mean values of the factor at stake.

Stress-inducing and stress-mitigating factors were standardized using two respective membership functions $\mu_{stress}(x)$ (Equation (1)) and $\mu_{resilient}(x)$ (Equation (2)) that depict the level to which the factor pertains to a fuzzy set:

$$\mu_{stress}(x) = \begin{Bmatrix} 1, x \leq x_a \\ 1 - 2 \times \left(\frac{x - x_b}{x_b - x_a}\right)^2, x_a \leq x \leq \frac{x_a + x_b}{2} \\ 2 \times \left(\frac{x - x_a}{x_b - x_a}\right)^2, \frac{x_a + x_b}{2} \leq x \leq x_b \\ 0, x \geq x_b \end{Bmatrix} \quad (1)$$

$$\mu_{resilient}(x) = \begin{Bmatrix} 0, x \leq x_a \\ 2 \times \left(\frac{x - x_a}{x_b - x_a}\right)^2, x_a \leq x \leq \frac{x_a + x_b}{2} \\ 1 - 2 \times \left(\frac{x - x_b}{x_b - x_a}\right)^2, \frac{x_a + x_b}{2} \leq x \leq x_b \\ 1, x \geq x_b \end{Bmatrix} \quad (2)$$

Following the standardization of the 17 exogenous factors, two single composite maps were firstly created to spatially represent the exogenous socio-economic and the coral buffering resilience.

The exogenous socio-economic composite layer was computed by summing the four stress and the single resilient layers:

$$\text{Resilience}_{\text{Exogeneous Socio-Economic}} = \sum_{i=1}^{4} \mu_{stress\ i} + \mu_{resilient\ j} \quad (3)$$

where $\mu_{stress\ i}$ is the membership value for the i^{th} layer, i = acute climatic hazards, acute oceanic hazards, acute chronic hazards, chronic oceanic hazards, $\mu_{resilient\ j}$ is the membership value for the j^{th} layer, and j = elevation resistance to oceano-climatic hazards.

In parallel, the coral buffering layer was built by (1) summing the six stress and the six resilient, and (2) multiplying the sum by the coral buffering layer:

$$\text{Resilience}_{\text{Coral Buffering}} = Coral\ buffering \times \left(\sum_{k=1}^{6} \mu_{stress\ k} + \sum_{l=1}^{5} \mu_{resilient\ l}\right) \quad (4)$$

where $\mu_{stress\ k}$ is the membership value for the k^{th} layer, k = thermal, sediment, urbanization, fishery, algal, emersion stressors, $\mu_{resilient\ l}$ is the membership value for the l^{th} layer, and l = connectivity, coral-source, habitat-sink, ecological-niche, cooling and coral-sink protection mitigators.

In a second step, two new single composite maps were calculated for the exogenous socio-economic and the coral buffering resilience by weighting each of the 17 fuzzied layers as a function of their contribution to the resilience. The 17 weights were gleaned from the literature and reported in the appropriate columns of the Tables 1 and 2. The weighting helped analyze time-averaged patterns across the archipelago.

3. Results

3.1. Socio-Economic and Ecological Regional Mapping

Analyses of the spatial SEE resilience during 2002–2012 indicated that both the coastal society and the coastal protection provided by coral reefs in the northern and southern study areas exhibited highly variable and distinct spatio-temporal patterns (Figures 4–6).

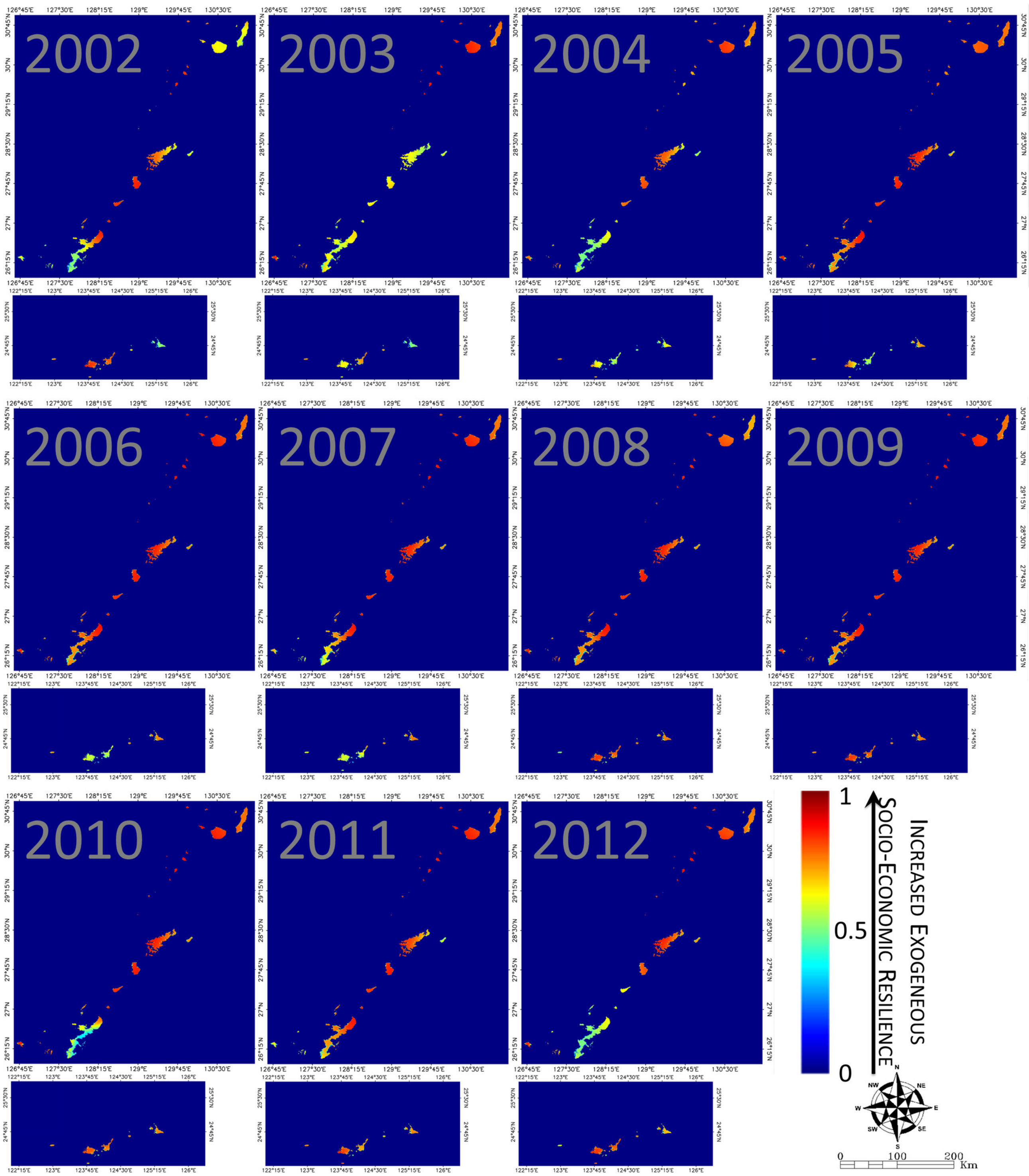

Figure 4. Nansei maps of the exogenous socio-economic resilience during 2002–2012. The resilience index was based on a suite of combined oceano-climatic and elevation factors using a fuzzy logic approach. For each year, the investigation of the Nansei region focused on the northern and southern parts (see the two study areas in Figure 1).

Except for 2002 and 2003, the low values (<0.7) of exogenous socio-economic resilience in the northern area (see Figure 1) were located at the southernmost island of Okinawa (Figure 4). In 2002 and 2003, in addition to Okinawa Island, low resilience values were found over the northeastern-most islands (Osumi sub-archipelago) and the middle islands (Amami sub-archipelago), respectively. In the southern study area, the lowest values were associated with the Miyako sub-archipelago from 2002–2004, as well as the Yaeyama sub-archipelago from 2003–2007. The spatial patterns of the average of the population (2000, 2005 and 2010) and the land price (2002 to 2012, yearly) revealed a large spatial correlation across the study region (Figure 5A, B, respectively). The most populated and wealthy areas were located on Okinawa Island, the Amami and Osumi sub-archipelagoes, and the Miyako and Ishigaki Islands. Juxtaposing the exogenous socio-economic resilience trend with the population/asset maps clearly indicated that the least resilient areas matched the most populated/wealthy areas, as exemplified by Okinawa and, to a lesser degree, the Miyako and Ishigaki Islands.

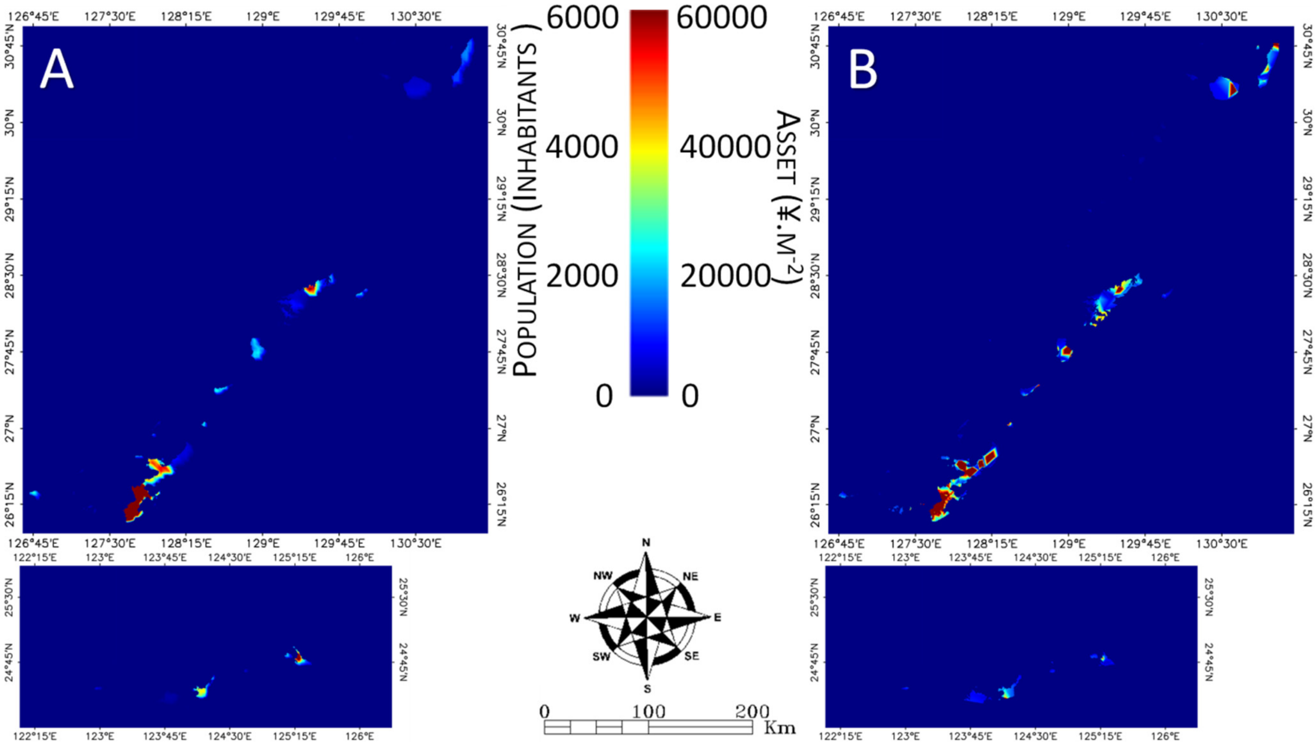

Figure 5. Nansei maps of the time-averaged (**A**) population (2000, 2005 and 2010), and (**B**) asset (2002–2012, yearly) endogenous socio-economic factors. The population is the trivial number of inhabitants, while the asset variable is represented by the land price (¥·m^{-2}).

Coral buffering resilience could be defined by a consistent spatial pattern during 2002–2012 (Figure 6). From south to north in the study region, the resilience decreased: it was highest in the Sekisei lagoon and Yaeyama sub-archipelago, moderate in the Okinawa sub-archipelago and lowest northward of the Amami sub-archipelago. A visual inspection of the coral buffering and exogenous socio-economic time series, along with the population/asset maps, suggested that high and moderate values of coral buffering resilience around Southwest Ishigaki, northern Miyako and the southern Okinawa Islands geographically coincided with areas with moderate and high socio-economic vulnerability, respectively (*i.e.,* moderate and low exogenous socio-economic resilience corresponded with high population/asset).

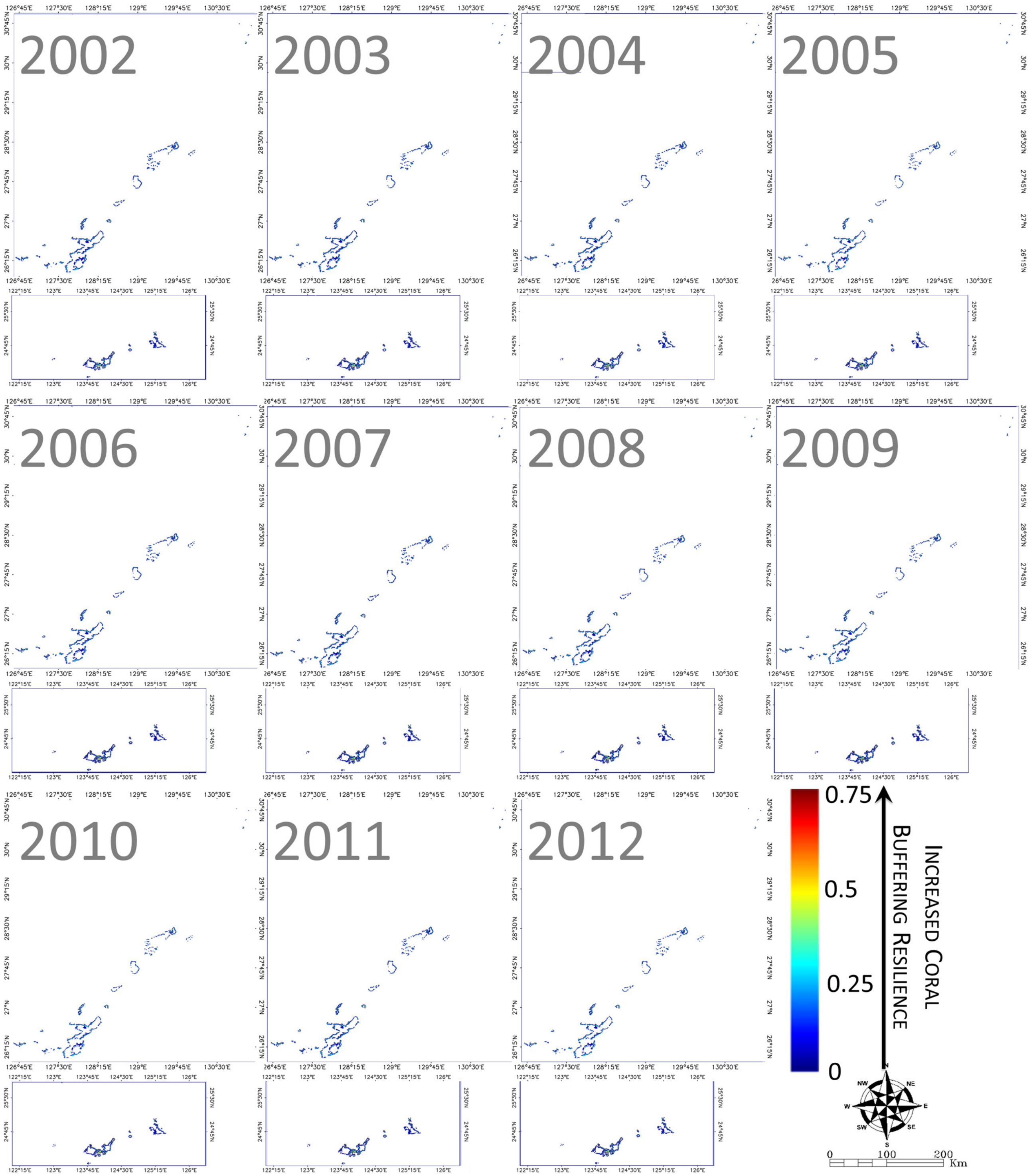

Figure 6. Nansei maps of coral buffering resilience during 2002–2012. The resilience index was based on a suite of combined thermal, sediment, urbanization, fishery, algal, emersion stressors; and connectivity, coral-source, habitat-sink, ecological-niche, cooling, coral-sink protection mitigators using a fuzzy logic approach. For each year, the investigation of the Nansei region focused on the northern and southern regions (see the two study areas in Figure 1).

3.2. Local Socio-Economic and Ecological Patterns

The representation of the SEE resilience time series using an island-averaged bubble plot, which is colored according to the sub-archipelago and sized according to the population/asset, increased the ability to distinguish the spatial patterns of resilience among islands across the entire study region while preserving the geographic relationships (Figures 7 and 8).

The population attribute showed that populated islands (*i.e.,* Okinawa, Miyako and Ishigaki) were more likely to exhibit lower values of both exogenous socio-economic and coral buffering resilience during 2002–2012 (Figure 7). Conversely, islands with small populations tended to show high values of exogenous socio-economic resilience but were more widespread along the gradient of coral buffering resilience, which is negatively correlated with the latitudinal gradient.

The asset attribute visually translated the positive logarithmic relationship of the SEE resilience in a superior manner because of the more evenly distributed wealth across the Nansei archipelago (compared with the population distribution) (Figure 8).

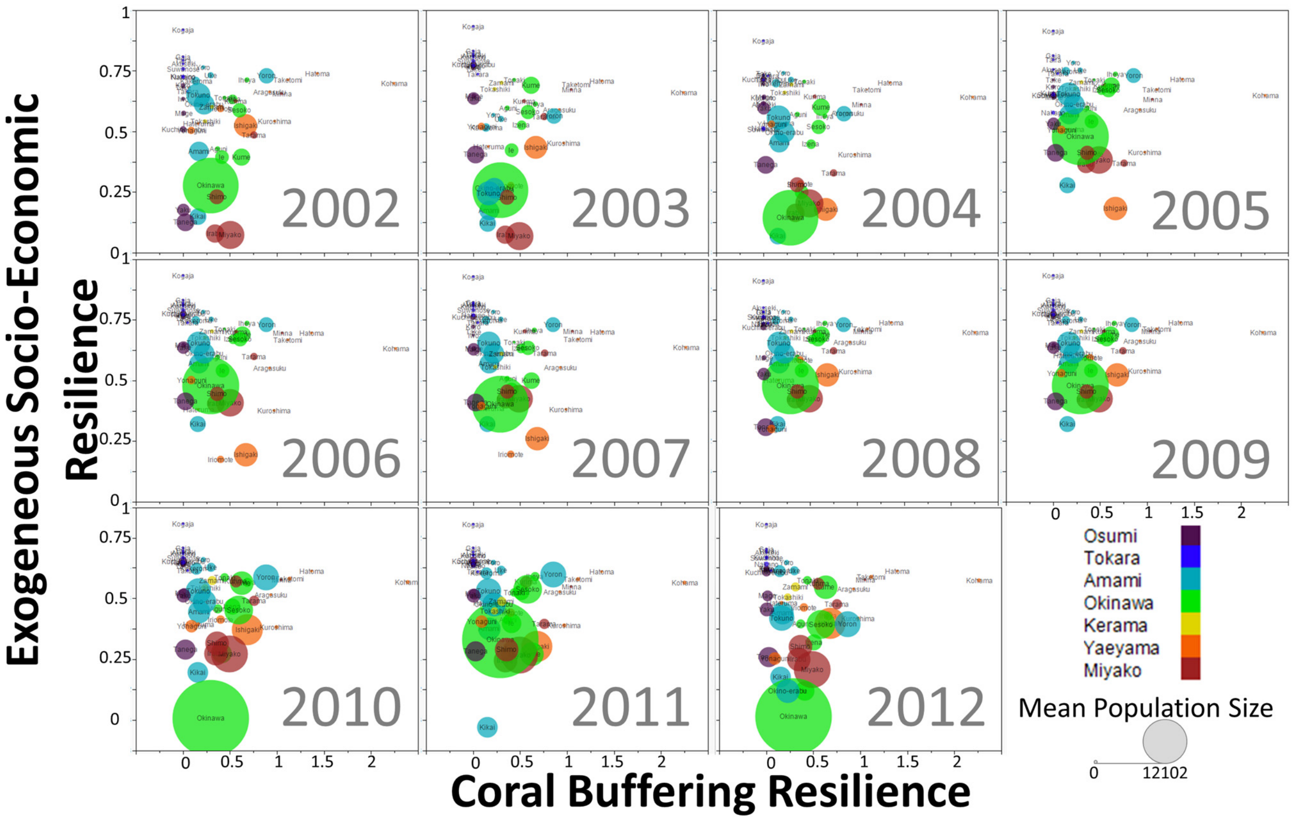

Figure 7. Island-scale bubble plots of the exogenous socioeconomic resilience with the coral buffering resilience. The bubble size represents the mean population, and the colors represent the Nansei sub-archipelagoes during 2002–2012.

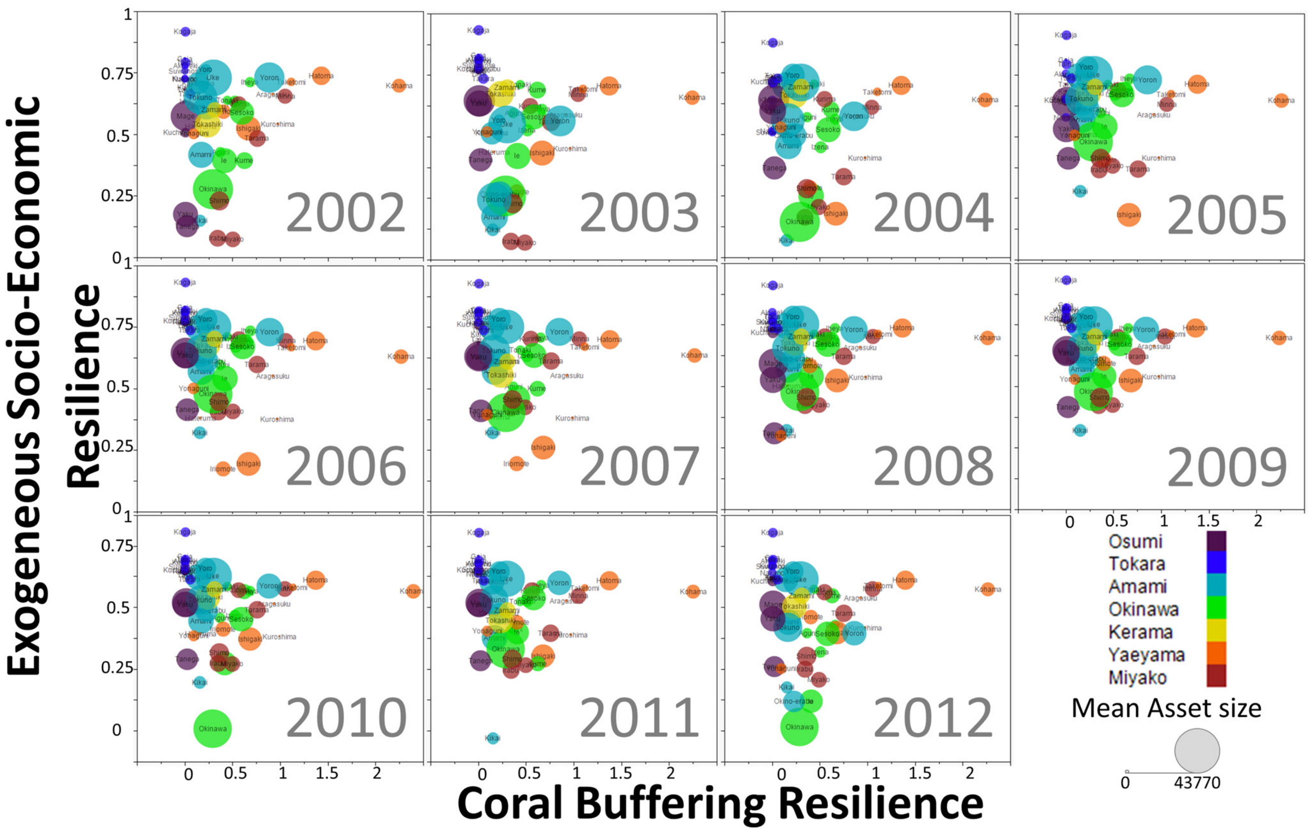

Figure 8. Island-scale bubble plots of the exogenous socioeconomic resilience with the coral buffering resilience. The bubble size represents the mean asset (¥·m^{-2}), and the colors represent the Nansei sub-archipelagoes during 2002–2012.

Other interesting patterns common to both the population and asset but difficult to interpret from the maps are as follows. The coral buffering resilience of the Osumi/Tokara-attached islands was consistently low, irrespective of the exogenous socio-economic resilience. The SEE resilience of the small islands of the Yaeyama archipelago (*i.e.*, islands included in Sekisei lagoon) was high, and the geographically remote islands (e.g., the southwestern-most Yonaguni and northeastern-most Tanega islands) were dynamically linked. A temporal analysis of the bubble behaviors (apparent using an animation) highlighted obvious shifts in the SEE resilience over the decade manifested along the exogenous socio-economic axis in the form of rebounds and, to a lesser extent, along the coral buffering axis in the form of slight oscillations, particularly for higher values.

4. Discussion

The results synthesized in this study represent the first spatial assessment of Japanese coral reefscapes, which intertwine socio-economic and ecological (SEE) systems. Endowed with high spatial accuracy and extent, this assessment was guided by the concept of resilience. Resilience was first examined at exogenous socio-economic and ecological organizational scales and was secondly examined at the integrated SEE scale, which focused on the coastal protection service provided to humans by coral reefs. Based on freely available spatially explicit data, we determined the resilience of three components (population/asset/coral buffering) by identifying the stress-inducing and stress-mitigating factors from the relevant literature and by linking the factors using fuzzy logic suitable for modeling complex systems.

4.1. Factor Selection and Recommendations

The spatial ensemble implemented in this study was based on factors that meet the criteria for their relevance to resilience, spatio-temporal continuity, quantity and quality, and affordability.

The resilience of the socio-economic component targeted population and asset values as proxies of the human sub-system. Beyond the key factor of population, the exposure of the asset value is critical in decision-making processes that focus on coastal management and ongoing climate change [63]. The land price (in ¥·m^{-2}) was selected as the proxy for the asset value given its basic correlation between economic valuation and spatial coverage and its annual values over the period of interest. Although the land price offers a synthetic capital appraisal of the direct losses (*i.e.,* stock) in case of flooding, the insured structure and contents (by residential, commercial and industrial sectors), as well as the indirect losses (*i.e.,* flow), might refine and complement the overall costs [64]. The outcome of the relationships between both the magnitude and return period of cyclone/tsunami and extreme water levels is ongoing research that could be relevantly combined with IPCC-predicted sea levels (IPCC 5th Assessment Report) to produce meaningful flood risk analyses.

The factors that underlie the assessment of coral buffering resilience were found in the referential body of literature [12,15]. We screened the cited indicators according to the availability of free data, which should have an appropriate spatial coverage and resolution and a substantial time series when possible. Of the 12 resilience sectors cited by [15] and ranked by [12], we managed to spatialize (*i.e.,* rasterize) eight at 1 arcsec spatial resolution. The remaining four sectors depicting coral and fish populations were not included because they require additional effort in processing the spatial resolution (*i.e.,* <5 m) [17], which is only useful for localized studies at present.

The SEE resilience was mapped over a regional area at a fine resolution and over one decade with a one year lag. For transferability, we aimed to find freely available data sourced from non-governmental, inter-governmental, and governmental institutions, as well as low-cost data, *i.e.*, commercial products provided by Google Earth. Both the fishery pressure and bathymetric complexity were derived from the Google Earth image database. The Google Earth archive contains high- and very-high-resolution spatial and temporal data that may be used as georeferenced multispectral data following a customized and easy-to-transfer procedure [62]. Because of the temporal data available for particular factors, we computed the resilience indicators from 2002–2012 while maintaining temporally static data values for the factors that do not differ from one year to next due to their coarse temporal resolution. An intuitive but insightful pattern emerged from the analysis of the consistency in the temporal computation: there is a trade-off (negative exponential relationship) between the spatial and temporal resolution (Figure 9). Despite its current Cartesian coordinates (Figure 8), Google Earth continues to provide data at a very high pixel size, but the pixels are often aggregated to an annual resolution. Notably, the temporal resolution of these detailed images is significantly greater in developed countries [65].

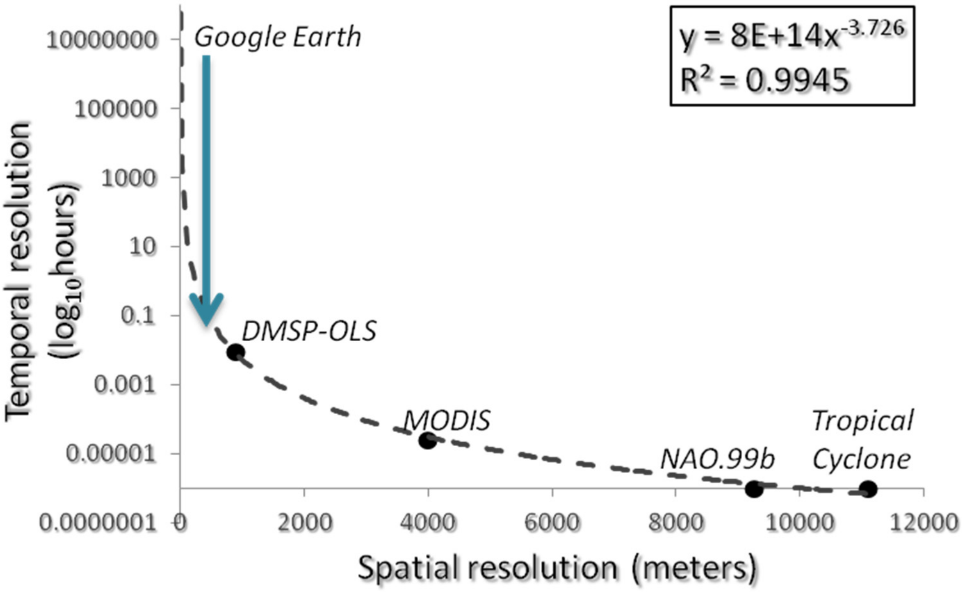

Figure 9. Relationship between the spatial resolution of some investigated factors and the natural logarithm of their temporal resolution. The arrow shows the current Google Earth trend of refining the temporal resolution while maintaining the same high spatial resolution.

4.2. Representing the Socio-Economic and Ecological Resilience

This study pioneers resilience mapping by coupling the SEE components of an integrated coastal system. This task was accomplished by adopting a circumspect and pragmatic approach in which the resiliencies of the SEE components were first addressed separately; then, the seamless SEE system was analyzed. The linkage between the two sub-systems was assured by the coastal protection provided by coral reefs to the human population. We mainly focused on the exposure, hazards and resistance of the system, rather than the adaptive capacity, such as the public emergency service [66], the coral memory of thermal tolerance [67], or the willingness of the population to adopt coastal ecosystem-based management [68]. By including factors tied to adaptive capacity, the system trajectories can be refined in the context of climate change via merging the assessment of transformation, self-organization and renewal to the conventional vulnerability framework.

Mapping the SEE resilience at 1 arcsec (30 m) suggested that coral buffering resilience negatively correlates with latitude. However, the ecological representation of the spatial resilience, contrary to the socio-economic aspect, was confined to areas whose sizes precluded a satisfactory visual appreciation over a regional site (see Figure 6). Considering the spatial resilience was computed as a time series, a synoptic but accurate representation was needed to overcome the coarsely qualitative map examination. The island-averaged, sub-archipelago-colored bubble plot (see Figures 7 and 8) confirmed the tendencies observed in the exogenous, endogenous socio-economic and coral buffering maps (Figures 4–6, respectively) and revealed insightful patterns that were previously overshadowed. Beyond targeting whether islands were resilient, as the maps determined, the bubble plot showed that a higher island population corresponds to a smaller and narrower SEE resilience (Figure 10A) and that the asset did not vary with the SEE resilience (Figure 10B). The latter observation was not clearly rendered in the related maps and implied an absence of correlation between the proxy for asset values and the SEE resilience.

The corollary implied that a regime shift in the investigated resilience would reasonably affect economic goods and services at the same magnitude, regardless of the geographic location within the Nansei archipelago.

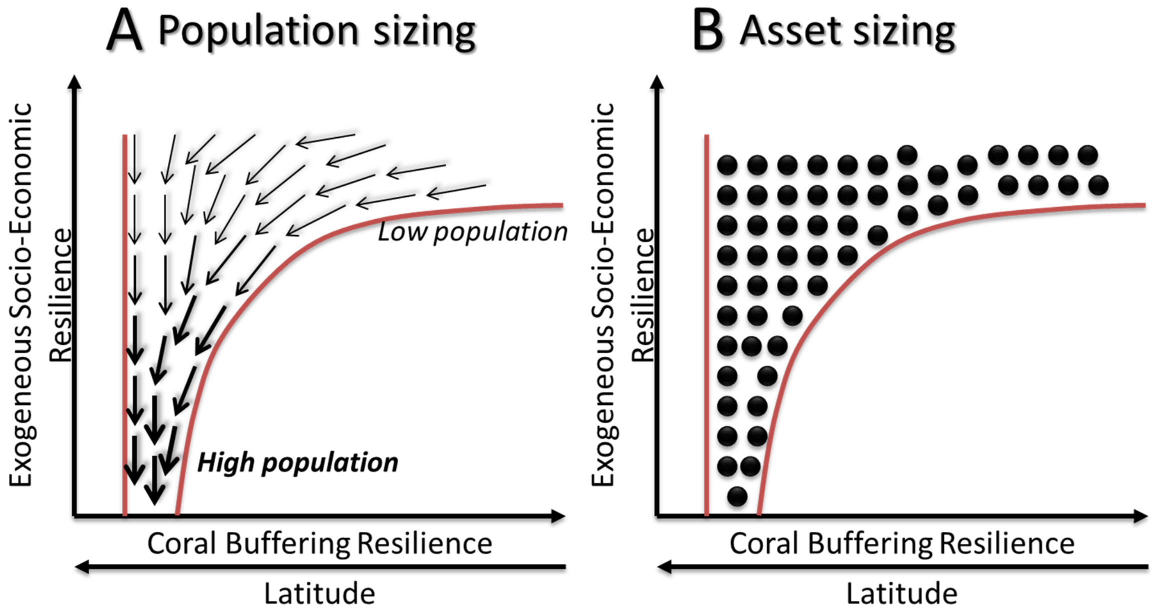

Figure 10. Conceptual interpretation of the SEE resilience bubble plot weighted by (**A**) the population amount and (**B**) the asset value (*i.e.,* land price in ¥ m^{-2}). The red lines symbolize the boundaries of the distribution; the thickness of the arrow is positively correlated with the population size; and the spatial uniformity of the circles represents the absence of correlation with the SEE distribution.

4.3. Guidance Implications

The temporal patterns of the bubble plots fit the oscillations of the island-averaged values of the SEE resilience. Because of the higher temporal variability observed over the decade, we could deduce that an 11-year period is better suited to capture and study the exogenous socio-economic variability than the coral buffering variability. Given the substantial amount of factors included in this study, it is difficult to explain the source(s) of the detected oscillations. A finer selection of factors coupled with a sensitivity analysis would help the interpretation of these patterns. A factor-weighted (see Tables 1 and 2) bubble plot averaged across the examined decade was computed for the population (Figure 11A) and for the asset value (Figure 11B) exposure to provide meaningful and necessary information for relevant guidelines:

Despite the highlighted bound between high populations and low SEE resilience, the island that exhibited the poorest resilience, Kikai (Amami sub-archipelago, #1 in Figure 11C), does not contain a large population. This very low resilience spot, which is an eastern location that experiences Pacific Ocean hazards (typhoons and tsunamis) and that features a low elevation resistance and narrow coral reef stripes, should be prioritized for ecosystem-based management.

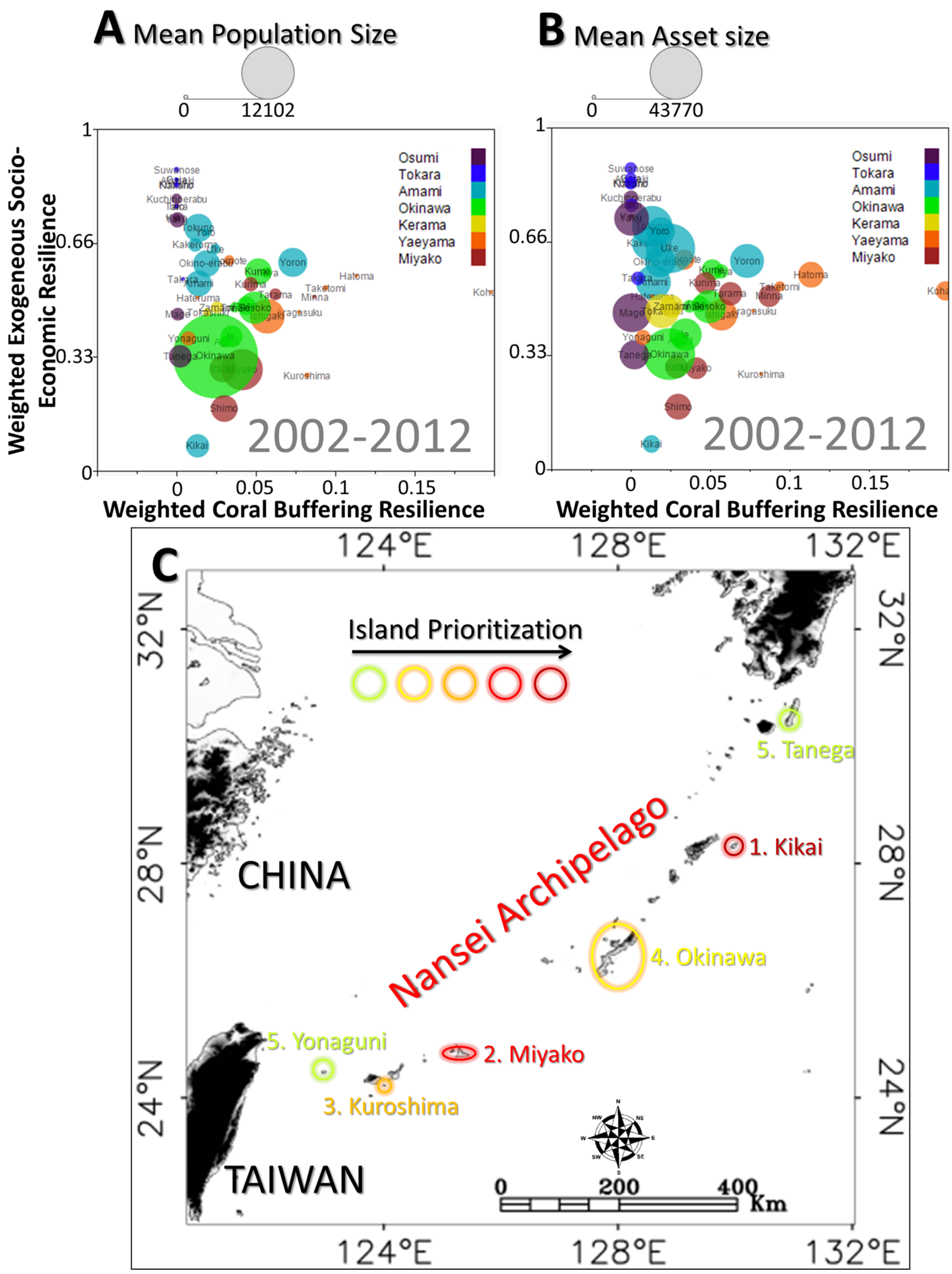

Figure 11. Island-scale bubble plots of the (**A**) population-sized and (**B**) asset-sized exogeneous socio-economic resilience with the coral buffering resilience as weighted by the factor influences found in the literature and colored by the Nansei sub-archipelagoes for 2002–2012. (**C**) Nansei map of coastal management prioritization.

The three eastern-most islands of the Miyako sub-archipelago (*i.e.,* Shimo, Miyako and Irabu, #2 in Figure 11C) are characterized by a slightly higher SEE resilience, which is mainly caused by the three factors mentioned for Kikai, as follows. Endowed with an enhanced coral buffering resilience but similar exogenous socio-economic resilience, Kuroshima (Yaeyama sub-archipelago, #3 in Figure 11C) has a low population but has the same three constraints. Therefore, the risks inherent to the southern islands of both the Miyako and Yaeyama sub-archipelagoes should be anticipated. This caveat is moreover corroborated by past events, such as the 7.5 tsunami in 1771, which caused approximately 12,000 deaths in the southern areas of these two sub-archipelagoes (Global Historical Tsunami Database).

Okinawa Island (#4 in Figure 11C) should be particularly targeted because of its relatively low SEE resilience and very high population exposure. Interestingly, the resilience values of the southwestern-most Yonaguni and northeastern-most Tanega Islands (#5 in Figure 11C) are very close to Okinawa Island, which is located in the middle of the Nansei archipelago. From this counterintuitive observation, we advocate that the overarching guidelines of an efficient ecosystem-based management of Japanese reefscapes may be applied to any islands along the latitudinal gradient. In the context of ocean warming and the northward migration of marine populations, implementing a management plan of the northern-most shallow coral reefs in the Northern Hemisphere, *i.e.,* in Tanega, where spatially restrained but healthy scleractinian-regime reefs exist, is highly recommended (Collin, pers. comm.).

Finally, the high SEE resilience exhibited by the Yaeyama Islands, including the Sekisei Lagoon (*i.e.,* the largest lagoon in Japan), heavily promotes the protective symbiosis between the human population and coral reefs and the continuing the efforts undertaken at the lagoon scale (*i.e.,* Iriomote-Ishigaki National Park) and the island scale (*i.e.,* the Kuroshima Kyanguch marine park, the Aragasuku-jima Maibishi marine park, and the Taketomi-jima Shimobishi and Takedonguchi marine parks).

4.4. Limitations

The output of the presented model is subject to the assignation of the membership functions. Misunderstanding the SEE response to exogenous factors may strongly limit the accuracy of spatial modeling. For instance, tide exposure, as a proxy for emersion, was used as a stress-inducing factor and was subsequently modeled using a decreasing logistic function, as advocated by [48]. However, daily tidal fluctuations might enhance adaptive mechanisms, which may increase coral resilience to a punctual acute disturbance, such as sea warming or desalination. In contrast, thermal cooling, represented by the occurrence of upwelling, was considered a stress-mitigating factor; thus, we used the increasing logistic function, as recommended by [56]. Nevertheless, in the Nansei region, where the northernmost shallow coral reefs exist, the contact of coral reefs with cold water (*i.e.,* <18 °C) may be detrimental to particular coral species.

Although the specificities and complementarities of the maps and innovative plots employed in this study described the reefscape resilience processes, the 1 arcsec map was not appropriate to embody the <1 km size coral buffering resilience at the regional scale. Additionally, the bubble plot degraded the geographic accuracy of large islands because of the averaging process. A rigorous spatial interpolation was applied to the coarsely gridded data to reach a standardized 1 arcsec accuracy, and factors were selected for their annual resolution; however, the aggregation of the data featured with various spatio-temporal specificities generated uncertainty due to discrepancies in the spatio-temporal correlation structure [69].

5. Conclusions

Despite the limitations and improvements discussed above, the SEE resilience tied to coral reefs was, for the first time, regionally mapped (1200 km) at a fine resolution (1 arcsec) over a decade (11 years). Through the established framework, we combined multi-source, multi-date, and spatially explicit data into a complex time series that elucidated spatial patterns of coastal human population and asset risks in Japan and of the coral reef barrier that mitigates these risks. The 11-year analysis better captured the variability in the exogenous socio-economic resilience than in the coral buffering resilience. Once the factors were weighted according to their resilience contributions, temporally static patterns emerged: (1) a negative correlation existed between coral buffering resilience and latitude; (2) the least resilient islands are low-lying, deprived of wide reef barriers, and located on the eastern and southern boundaries of the Nansei archipelago; (3) the southwestern-most, middle and northeastern-most islands have the same SEE resilience; and (4) Sekisei Lagoon islands have a very high coral buffering resilience. To overcome uncertainty, future studies should focus on the socio-ecological adaptive capacity, fine-scale ecological processes (such as coral and fish functional groups) and predictions of flood risks for the coming decades.

Acknowledgments

This research was fully supported by Grant-in-Aid for JSPS Fellows (No. 2402800) of the Japan Society of the Promotion of Science (JSPS) and was partially supported by Grant-in-Aid for Scientific Research (A) (Nos. 24246086 and 25257305) of JSPS. The authors deeply acknowledge both anonymous reviewers who assist in greatly improving the manuscript.

Author Contributions

Antoine Collin mainly conducted the research and writing related to this manuscript. Lawrence Bernardo led the tidal hindcast ending with the emersion adjustment factor. Kazuo Nadaoka supervised the research and writing related to this manuscript.

Conflicts of Interest

The authors declare no conflicts of interest.

References

1. Barbier, E.B.; Hacker, S.D.; Kennedy, C.; Koch, E.W.; Stier, A.C.; Silliman, B.R. The value of estuarine and coastal ecosystem services. *Ecol. Monogr.* **2011**, *81*, 169–193.
2. Costanza, R.; de Groot, R.; Sutton, P.; van der Ploeg, S.; Anderson, S.J.; Kubisszewski, I.; Farber, S.; Turner, R.K. Changes in the global value of ecosystem services. *Global Environ. Chang.* **2014**, *26*, 152–158.
3. Wilkinson, C. *Status of Coral Reefs of the World*: *2008*; Global Coral Reef Monitoring Network and Reef and Rainforest Research Center: Townsville, QLD, Australia, 2008; p. 298.
4. Bellwood, D.R.; Hughes, T.P.; Folke, C.; Nystrom, M. Confronting the coral reef crisis. *Nature* **2004**, *429*, 827–833.
5. Hoegh-Guldberg, O.; Mumby, P.J.; Hooten, A.J.; Steneck, R.S.; Greenfield, P.; Gomez, E.; Harvell, C.D.; Sale, P.F.; Edwards, A.J.; Caldeira, K.; *et al.* Coral reefs under rapid climate change and ocean acidification. *Science* **2007**, *318*, 1737–1742.
6. Nyström, M.; Folke, C. Spatial resilience of coral reefs. *Ecosystems* **2011**, *4*, 406–417.

7. McClanahan, T.; Polunin, N.; Done, T. Ecological states and the resilience of coral reefs. *Conserv. Ecol.* **2002**, *6*, 18.
8. Mumby, P.J.; Hastings, A.; Edwards, H.J. Thresholds and the resilience of Caribbean coral reefs. *Nature* **2007**, *450*, 98–101.
9. Roff, G.; Mumby, P.J. Global disparity in the resilience of coral reefs. *Trends Ecol. Evol.* **2012**, *27*, 404–413.
10. Nyström, M.; Graham, N.A.J.; Lokrantz, J.; Norström, A.V. Capturing the cornerstones of coral reef resilience: Linking theory to practice. *Coral Reefs* **2008**, *27*, 795–809.
11. Hughes, T.P.; Graham, N.A.; Jackson, J.B.; Mumby, P.J.; Steneck, R.S. Rising to the challenge of sustaining coral reef resilience. *Trends Ecol. Evol.* **2010**, *25*, 633–642.
12. Maynard, J.A.; Marshall, P.A.; Johnson, J.E.; Harman, S. Building resilience into practical conservation: Identifying local management responses to global climate change in the southern Great Barrier Reef. *Coral Reefs* **2010**, *29*, 381–391.
13. McClanahan, T.R.; Donner, S.D.; Maynard, J.A.; MacNeil, M.A.; Graham, N.A.J.; Maina, J.; Baker, A.C.; Alemu I., J.B.; Beger, M.; Campbell, S.J.; *et al.* Prioritizing key resilience indicators to support coral reef management in a changing climate. *PLoS ONE*. **2012**, *7,* e42884.
14. Mumby, P.J.; Wolff, N.H.; Bozec, Y.-M.; Chollett, I.; Halloran, P. Operationalizing the resilience of coral reefs in an era of climate change. *Conserv. Lett*. **2014**, *7*, 176–187.
15. Obura, D.; Grimsditch, G. *Resilience Assessment Of Coral Reefs—Assessment Protocol For Coral Reefs, Focusing On Coral Bleaching And Thermal Stress*; IUCN: Gland, Switzerland, 2009.
16. Maina, J.; McClanahan, T.R.; Venus, V.; Ateweberhan, M.; Madin, J. Global gradients of coral exposure to environmental stresses and implications for local management. *PLoS ONE*. **2011**, doi: 10.1371/journal.pone.0023064.
17. Knudby, A.; Jupiter, S.; Roelfsema, C.; Lyons, M.; Phinn, S. Mapping coral reef resilience indicators using field and remotely sensed data. *Remote Sens*. **2013**, *5*, 1311–1334.
18. Rowlands, G.; Purkis, S.; Riegl, B.; Metsamaa, L.; Bruckner, A.; Renaud, P. Satellite imaging coral reef resilience at regional scale. A case-study from Saudi Arabia. *Mar. Pollut. Bull.* **2012**, *64*, 1222–1237.
19. Folke, C. Resilience: The emergence of a perspective for social-ecological systems analyses. *Glob. Environ. Chang*. **2006**, *16*, 253–267.
20. Folke, C.; Jansson, Å.; Rockström, J.; Olsson, P.; Carpenter, S.R.; Chapin, F.S., III.; Crépin, A.-S.; Daily, G.; Danell, K.; Ebbesson, J.; *et al*. Reconnecting to the biosphere. *Ambio* **2011**, *40*, 719–738.
21. Gao, L.; Hailu, A. Evaluating the effects of area closure for recreational fishing in a coral reef ecosystem: The benefits of an integrated economic and biophysical modelling. *Ecol. Econ.* **2011**, *70*, 1735–1745.
22. Melbourne-Thomas, J.; Johnson, C.R.; Aliño, P.M.; Geronimo, R.C.; Villanoy, C.L.; Gurney, G.G. A multi-scale biophysical model to inform regional management of coral reefs in the western Philippines and South China Sea. *Environ. Model. Softw*. **2011**, *26*, 66–82.
23. Gao, L.; Hailu, A. Ranking management strategies with complex outcomes: An AHP-fuzzy evaluation of recreational fishing using an integrated agent-based model of a coral reef ecosystem. *Environ. Model. Softw.* **2012**, *31*, 3–18.

24. Adger, W.N.; Hughes, T.P.; Folke, C.; Carpenter, S.R.; Rockström, J. Social-ecological resilience to coastal disasters. *Science* **2005**, *309*, 1036–1039.
25. Levin, S.A.; Lubchenco, J. Resilience, robustness, and marine ecosystem-based management. *Bioscience* **2008**, *58*, 27–32.
26. Cumming, G.S. Spatial resilience: Integrating landscape ecology, resilience, and sustainability. *Landsc. Ecol*. **2011**, *26*, 899–909.
27. Cumming, G.S.; Bodin, O.; Ernstson, H.; Elmqvist, T. Network analysis in conservation biogeography: Challenges and opportunities. *Divers Distrib.* **2010**, *16*, 414–425.
28. Zadeh, L.A. The concept of a linguistic variable and its application to approximate reasoning. *Inf. Sci.* **1965**, *8*, 199–249.
29. Mann, K.H.; Lazier, J.R.N. *Dynamics of Marine Ecosystems*, 2nd ed.; Blackwell Publishers: Oxford, UK, 2006.
30. *Area of Japanese Prefectures as of October 1, 2011*; Statistics Bureau of Japan: Tokyo, Japan, 2011.
31. Annual Report of the Regional Specialized Meteorological Center Tokyo—Typhoon Center. Available online: http://www.jma.go.jp/jma/jma-eng/jma-center/rsmc-hp-pub-eg/RSMC_HP.htm (accessed on 10 June 2014).
32. Cover, Introduction, Earthquakes around the World, Earthquakes in and around Japan. Available online: http://www.jma.go.jp/jma/en/Activities/jishintsunami/jishintsunami_low1.pdf (accessed on 10 June 2014).
33. Smith, K. *Environmental Hazards: Assessing Risk and Reducing Disaster*, 6th ed.; Routledge: London, UK, 2013.
34. Geist, E.L.; Parsons, T. Probabilistic analysis of tsunami hazards. *Nat. Hazards* **2006**, *37*, 277–314.
35. Balica, S.F.; Wright, N.G.; van der Meulen, F. A flood vulnerability index for coastal cities and its use in assessing climate change impacts. *Nat. Hazards* **2012**, 1–33.
36. Hughes, T.P.; Baird, A.H.; Bellwood, D.R.; Card, M.; Connolly, S.R.; Folke, C.; Roughgarden, J. Climate change, human impacts, and the resilience of coral reefs. *Science* **2003**, *301*, 929–933.
37. Baker, A.C.; Starger, C.J.; McClanahan, T.R.; Glynn, P.W. Coral reefs: Corals' adaptive response to climate change. *Nature* **2004**, *430*, 741–741.
38. Berkelmans, R.; van Oppen, M.J. The role of zooxanthellae in the thermal tolerance of corals: A "nugget of hope" for coral reefs in an era of climate change. *Proc. R. Soc. B: Biol. Sci*. **2006**, *273*, 2305–2312.
39. Brown, B.E.; Dunne, R.P. The environmental impact of coral mining on coral reefs in the Maldives. *Environ. Conserv.* **1988**, *15*, 159–165.
40. Shepherd, A.R.D.; Warwick, R.M.; Clarke, K.R.; Brown, B.E. An analysis of fish community responses to coral mining in the Maldives. *Environ. Biol. Fishes*. **1992**, *33*, 367–380.
41. Rogers, C.S. Responses of coral reefs and reef organisms to sedimentation. *Mar. Ecol. Prog. Ser*. **1990**, *62*, 185–202.
42. Fabricius, K.E. Effects of terrestrial runoff on the ecology of corals and coral reefs: Review and synthesis. *Mar. Pollut. Bull.* **2005**, *50*, 125–146.
43. Lirman, D. Competition between macroalgae and corals: Effects of herbivore exclusion and increased algal biomass on coral survivorship and growth. *Coral Reefs* **2001**, *19*, 392–399.

44. Mumby, P.J.; Dahlgren, C.P.; Harborne, A.R.; Kappel, C.V.; Micheli, F.; Brumbaugh, D.R.; Gill, A.B. Fishing, trophic cascades, and the process of grazing on coral reefs. *Science* **2006**, *311*, 98–101.
45. McCook, L.J. Macroalgae, nutrients and phase shifts on coral reefs: Scientific issues and management consequences for the Great Barrier Reef. *Coral Reefs* **1999**, *18*, 357–367.
46. McCook, L.; Jompa, J.; Diaz-Pulido, G. Competition between corals and algae on coral reefs: A review of evidence and mechanisms. *Coral Reefs* **2011**, *19*, 400–417.
47. Brown, B.E. Adaptations of reef corals to physical environmental stress. *Adv. Mar. Biol*. **1997**, *31*, 222–301.
48. Anthony, K.R.N.; Kerswell, A.P. Coral mortality following extreme low tides and high solar radiation. *Mar. Biol.* **2007**, *151*, 1623–1631.
49. Roberts, C.M. Connectivity and management of Caribbean coral reefs. *Science* **1997**, *278*, 1454–1457.
50. Jones, G.P.; Almany, G.R.; Russ, G.R.; Sale, P.F.; Steneck, R.S.; van Oppen, M.J.H.; Willis, B.L. Larval retention and connectivity among populations of corals and reef fishes: History, advances and challenges. *Coral Reefs* **2009**, *28*, 307–325.
51. Berkelmans, R.; De'ath, G.; Kininmonth, S.; Skirving, W.J. A comparison of the 1998 and 2002 coral bleaching events on the Great Barrier Reef: Spatial correlation, patterns, and predictions. *Coral Reefs* **2004**, *23*, 74–83.
52. Mumby, P.J.; Dytham, C. Metapopulation dynamics of hard corals. In *Marine Metapopulations*; Kritzer, J.P., Sale, P.F., Eds.; Academic Press: Manhattan, NY, USA, 2006. pp. 157–203.
53. Pinsky, M.L.; Palumbi, S.R.; Andréfouët, S.; Purkis, S.J. Open and closed seascapes: Where does habitat patchiness create populations with high fractions of self-recruitment? *Ecol. Appl.* **2012**, *22*, 1257–1267.
54. Fabricius, K.E.; Mieog, J.C.; Colin, P.L.; Idip, D.; van Oppen, M.J.H. Identity and diversity of coral endosymbionts (zooxanthellae) from three Palauan reefs with contrasting bleaching, temperature and shading histories. *Mol. Ecol.* **2004**, *13*, 2445–2458.
55. McClanahan, T.R.; Maina, J.; Moothien-Pillay, R.; Baker, A.C. Effects of geography, taxa, water flow, and temperature variation on coral bleaching intensity in Mauritius. *Mar. Ecol. Prog. Ser.* **2005**, *298*, 131–142.
56. Manzello, D.P.; Brandt, M.; Smith, T.B.; Lirman, D.; Hendee, J.C.; Nemeth, R.S. Hurricanes benefit bleached corals. *Proc. Natl. Acad. Sci. USA* **2007**, *104*, 12035–12039.
57. McClanahan, T.R.; Marnane, M.J.; Cinner, J.E.; Kiene, W.E. A comparison of marine protected areas and alternative approaches to coral-reef management. *Curr. Biol*. **2006**, *16*, 1408–1413.
58. Ferrario, F.; Beck, M.W.; Storlazzi, C.D.; Micheli, F.; Shepard, C.C.; Airoldi, L. The effectiveness of coral reefs for coastal hazard risk reduction and adaptation. *Nat. Commun.* **2014**, doi:10.1038/ncomms4794.
59. Rogers, J.S.; Monismith, S.G.; Feddersen, F.; Storlazzi, C.D. Hydrodynamics of spur and groove formations on a coral reef. *J. Geophys. Res.: Ocean*. **2013**, *118*, 3059–3073.
60. Aubrecht, C.; Elvidge, C.D.; Longcore, T.; Rich, C.; Safran, J.; Strong, A.; Eakin, M.; Baugh, M.E.; Tuttle, B.T.; Howard, A.T.; *et al*. A global inventory of coral reef stressors based on satellite observed nighttime lights. *Geocarto Int.* **2008**, *23*, 467–479.

61. Matsumoto, K.; Takanezawa, T.; Ooe, M. Ocean tide models developed by assimilating TOPEX/POSEIDON altimeter data into hydrodynamical model: A global model and a regional model around Japan. *J. Oceanogr.* **2000**, *56*, 567–581.
62. Collin, A.; Nadaoka, K.; Nakamura, T. Mapping VHR water depth, seabed and land cover using Google Earth data. *ISPRS Int. J. Geo-Inf.* **2014**, *3*, 1157–1179.
63. Hallegatte, S.; Ranger, N.; Mestre, O.; Dumas, P.; Corfee-Morlot, J.; Herweijer, C.; Wood, R.M. Assessing climate change impacts, sea level rise and storm surge risk in port cities: A case study on Copenhagen. *Clim. Chang.* **2011**, *104*, 113–137.
64. Hallegatte, S. An adaptive regional input-output model and its application to the assessment of the economic cost of Katrina. *Risk Anal.* **2008**, *28*, 779–799.
65. Potere, D. Horizontal positional accuracy of Google Earth's high-resolution imagery archive. *Sensors* **2008**, *8*, 7973–7981.
66. Keim, M.E. Building human resilience: The role of public health preparedness and response as an adaptation to climate change. *Am. J. Prev. Med.* **2008**, *35*, 508–516.
67. Maynard, J.A.; Anthony, K.R.N.; Marshall, P.A.; Masiri, I. Major bleaching events can lead to increased thermal tolerance in corals. *Mar. Biol.* **2008**, *155*, 173–182.
68. Granek, E.F.; Polasky, S.; Kappel, C.V.; Reed, D.J.; Stoms, D.M.; Koch, E.W.; Wolanski, E. Ecosystem services as a common language for coastal ecosystem-based management. *Conserv. Biol.* **2010**, *24*, 207–216.
69. Burrough, P.; McDonnell, R. *Principles of Geographical Information Systems*; Oxford University Press: New York, NY, USA, 2005.